Population coding of movement dynamics by cerebellar Purkinje cells

Richard J. Krauzlis

Salk Institute for Biological Studies, 10010 North Torrey Pines Road, La Jolla, CA 92037, USA

Received 2 November 1999; accepted 27 January 2000

Acknowledgements: I thank Drs Thomas D. Albright, Stephen G. Lisberger, and Leland S. Stone for their comments on a previous version of this manuscript. R.J.K. is supported by NIH grant EY12212-01 and NASA grant NCC2-1024.

In order to accomplish desired movements, the nervous system must specify the movement dynamics: it must provide a signal that compensates for the mechanical constraints encountered during movement. Here we tested whether the population activity of Purkinje cells in the cerebellum specifies the dynamics for pursuit eye movements. We first estimated the population activity by computing weighted averages of Purkinje cell firing on a millisecond time scale. We then generated predicted eye movements by transforming this pooled neural activity with a description of eye mechanics. We found that the equally weighted average of Purkinje cell outputs produced a close match between the predicted and actual eye movements. These findings demonstrate that neural circuits through the cerebellum are capable of providing the dynamic compensation necessary to achieve desired movements. *NeuroReport* 11:1–6 © 2000 Lippincott Williams & Wilkins.

Key words: Cerebellum; Eye movements; Inverse dynamics; Oculomotor; Pursuit

INTRODUCTION

Pursuit eye movements, which primates use to smoothly track moving visual objects, depend critically upon the cerebellum [1]. In particular, the ventral paraflocculus and flocculus of the cerebellum provide a major component of the motor command for pursuit [2]. Purkinje cells in these regions exhibit large changes in simple-spike firing during pursuit eye movements [3–6] that is cosine-tuned for the direction of eye movement [7]. Figure 1 shows the simple-spike activity of four sample Purkinje cells (Fig. 1a) during the pursuit of a target that moved at a constant speed of 5 deg/s (Fig. 1b). When the eye starts moving, Purkinje cells exhibit a transient increase in firing rate as eye speed increases from zero toward target speed. As the eye movement continues, Purkinje cells exhibit a sustained, but lower, increase in firing rate while eye speed matches target speed.

Although it is known that the activity of these Purkinje cells is important for pursuit, the significance of the temporal variation in their firing rate has not been established. The firing rate of Purkinje cells varies as a function of eye speed, accounting for most of the sustained changes in activity observed during maintained pursuit [3–6]. However, this sensitivity to eye speed cannot account for the transient overshoots in firing rate during the initiation of pursuit, because the overshoots in firing are typically much larger than any overshoots in eye speed (Fig. 1). Previously, these overshoots have been attributed to either visual inputs [6,8] or an eye acceleration component to Purkinje cell firing [9]. The results we present here demonstrate that these transient overshoots in firing have the appropriate amplitude and timing, on average, to overcome the sluggish dynamics of the eye plant during the onset of pursuit.

MATERIALS AND METHODS

Protocol: We recorded from Purkinje cells ($n = 50$) in the ventral paraflocculus of two monkeys using standard recording and analysis techniques as described in detail previously [6,7]. Briefly, under halothane anesthesia and aseptic conditions, monkeys were implanted with a coil of wire in one eye for measuring eye movements, a head holder, and a recording cylinder. Extracellular potentials were recorded from Purkinje cells with glass-insulated platinum–iridium microelectrodes while the monkeys tracked the visual target to acquire liquid reinforcements. Monkeys were trained to smoothly follow a small target spot that was initially at rest and then started to move at a constant speed in the Purkinje cell's preferred direction. At the onset of target motion, a step displacement of the target was added to eliminate the need for the monkey to make corrective saccades.

Measures: For each Purkinje cell, we aligned the responses on the onset of target motion and averaged the simple-spike firing rates and eye velocity records from 20–30 trials. We measured overshoot indices for each Purkinje cell from its average simple-spike firing rate during three intervals: (1) baseline was measured in a 100 ms interval ending on target motion onset, (2) peak was measured in a 50 ms interval starting 125 ms after target motion onset, and (3) maintained was measured in a 150 ms interval

Article number = 9310

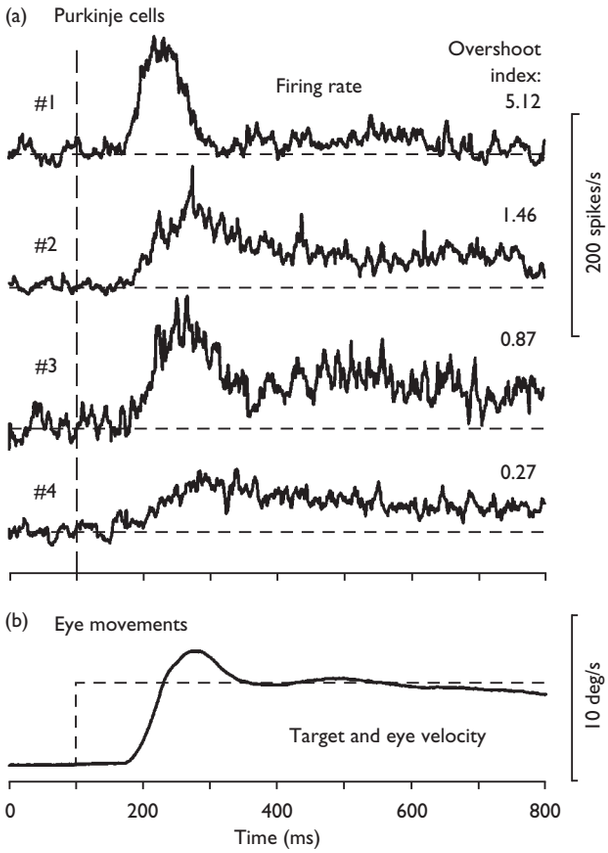

Fig. 1. Overshoots in the firing rate of Purkinje cells during pursuit eye movements. (**a**) The simple-spike firing of four Purkinje cells in the ventral paraflocculus during 20–30 presentations of a target moving at 5 deg/s in their preferred direction. Firing rates are aligned on target motion onset. Numbers to right of each trace indicate the individual overshoot indices for each Purkinje cell. (**b**) The target speed (gray) and average eye speed (solid) recorded at the same time as the four firing rates.

starting 350 ms after target motion onset. The overshoot index was defined as peak−baseline/maintained−baseline.

Analysis: Populations of firing rate were constructed by subtracting the baseline firing rate from each Purkinje cell, scaling the firing rate by a weight determined by eqn (2) in the Results section, and averaging across all Purkinje cells in 1 ms steps for the duration of the trial. In cases in which this scaling would have provided negative firing rates, the firing rate was assigned a value of zero instead. These population averages were then provided as inputs to a description of the eye plant. Simulations were run using the Matlab Simulink toolbox. Optimal fits were obtained by adjusting the w_o and/or w_s parameters of eqn (2) to minimize the squared error between predicted and actual eye speed. Estimates of the variance in predicted eye velocity for χ^2 tests were generated using a bootstrap procedure: optimal fits were obtained with 150–200 population averages, each made from Purkinje cells randomly selected from our sample (with replacement), to generate a distribution of predicted values at each time point.

Statistical tests were performed using commercially available software (SigmaStat, SPSS) and algorithms [10]. Other descriptions of some of the neuronal data used in this paper have been published previously [7,11].

RESULTS

It is possible to directly test whether these Purkinje cells provide dynamic compensation during pursuit movements, because the eye is a mostly linear mechanical system and the system dynamics can be inferred from the firing rates of ocular motor neurons [12,13]. A single set of ocular motor neurons is used for all classes of eye movements and their firing rates are generally related to eye movements as follows: $F_{MN}(t) = ke(t) + re'(t) + e''(t) - T_s F_{MN}(t)$ (1) where F_{MN} (t), e(t), e′(t) and e″(t) are the rate of motor neuron firing, the eye position, eye velocity, and eye acceleration at time t. Recordings from motor neurons have provided estimates of the typical values of the three coefficients: k (4 spikes/s/deg), r (0.95 spikes/s/(deg/s)), and m (0.015 spikes/s/(deg/s^2)) [12,13], which reflect the elastic, viscous, and inertial properties of the eye, respectively. In addition, the firing rates of motor neurons exhibit a slide component, T_s, described by a time constant of ~83 ms [14]. Changes in motor neuron firing directly change the forces applied to the eye; these forces are filtered by the dynamics of the eye plant to produce the physical movement of the eyes. In contrast to the limbs, the load imposed by the eyes is essentially constant, greatly simplifying the relationship between changes in the applied force and the resulting movements. Based upon eqn (1), the eye plant can be described as a second-order linear system with two poles ($T_1 = 16$ ms, ~m/r, and $T_2 = 179$ ms, ~r/k) and one zero (T_s s = 83 ms) [12,13]. More complex nonlinear models of the plant have been proposed to account for the faster dynamics of saccadic eye movements [15], but linear models like that based upon en (1), or even simpler, are generally used in descriptions of smooth eye movements [9,16].

Using this quantitative description of eye dynamics, we directly tested whether the population activity of the Purkinje cells in our sample ($n = 50$) provides adequate compensation for the eye plant. However, we did not know *a priori* the amplitude of the contribution that each Purkinje cell makes to the eye movement, because each may provide different numbers or strengths of synapses onto target neurons in the brain stem. It is also possible that our sample of Purkinje cells is biased toward those with particular temporal firing patterns. On the other hand, weighting the contribution of each Purkinje cell independently would create a large number of free parameters and, because many Purkinje cells have similar firing patterns, many of these parameters would be redundant. To constrain the number of parameters, we therefore parameterized the contribution of each Purkinje based upon the degree of overshoot exhibited during the initiation of pursuit. We quantified the degree of overshoot with an overshoot index, which represents the fractional overshoot in firing exhibited during pursuit onset (defined in the Measures section of Materials and Methods). For the population of Purkinje cells ($n = 50$) the mean overshoot index was 2.34 (± 4.49, s.d.), meaning that the average transient component was more than twice as large as the

sustained component, consistent with earlier findings [6,11]. We then scaled the contribution of each Purkinje cell to the population average by multiplying their firing pattern with a weight ($Weight_i$) determined by the equation: $Weight_i = w_o + w_s$ overshoot $index_i$ (2), where w_o and w_s define the intercept and slope, respectively, of a linear function with the overshoot index as the independent variable. This equation allowed us to smoothly grade the contribution of each Purkinje with just two free parameters.

Changes in the two parameters w_o and w_s defined different weighting schemes that produced very different estimates of the population average of Purkinje cell activity. Passing these population averages through the description of the eye plant, in turn, predicted eye movements with substantially different temporal profiles (Fig. 2). For example, a low weighting scheme ($w_s = -0.045$, $w_o = 0.35$) biased the population average toward those Purkinje cells with smaller or no overshoots and predicted an eye movement that undershoots the actual observed eye movement. A high weighting scheme ($w_s = 0.045$, $w_o = 0.35$) biased the population average toward Purkinje cells with larger overshoots and predicted an eye movement that overshoots the observed eye movement.

To determine the best weighting scheme, we adjusted w_o and w_s to minimize the difference between the predicted and actual eye movements. The resulting optimal weighting scheme ($w_s = 0.003$. $w_o = 0.370$) produced an excellent match between predicted and actual eye speed, as indicated by the determination coefficient (0.98) of the correlation between the two signals. Importantly, this optimal scheme weighted each Purkinje cell almost equally: that is, the value of w_s (0.003) was close to zero. When we imposed an explicitly equal weighting scheme ($w_s = 0.0$, $w_o = 0.376$; that is, the firing rate of each Purkinje cell was scaled by the same factor of 0.376 deg/s/(spikes/s)), we obtained a similar excellent match between predicted and actual eye speed (determination coefficient: 0.98). To determine whether this equal weighting scheme provided a good model of actual eye velocity, we compared the predicted and actual eye velocities using a χ^2 test. The resulting Q score (> 0.99) indicates that it is $< 1\%$ likely that the differences between the two sets of data were not due merely to chance. When we compared the predicted eye speed obtained with the equal weighting scheme to that produced with the optimal weighting scheme, we again found that the differences were probably due to chance ($Q > 0.99$). These results demonstrate that a population average of equally weighted Purkinje cells can compensate for eye dynamics during pursuit eye movements.

The match between predicted and actual eye speed is not an automatic consequence of the facts that the eye plant has sluggish dynamics and Purkinje cells exhibit a range of overshoots in firing rate. For example, the eye plant is sometimes described in a simpler form by omitting the zero term, T_s. This simplification ignores the slide component in the firing rate of ocular motor neurons [14,17] and reduces the eye plant to a low-pass filter. When we used this simpler description of the eye plant (Fig. 2), the weighted average of Purkinje cell firing provided a poor match between predicted and actual eye speed ($r^2 = 0.80$, $Q > 0.05$), even when the weighting scheme was optimized to produce the best fit ($w_s = 0.074$, $w_o = 0.24$).

To analyze the effect of plant dynamics more systematically, we tested the match between predicted and actual eye speed for a range of hypothetical alternative plants. Using a population average obtained by equally weighting each Purkinje cell (i.e. $w_s = 0.0$), we altered the time-constant parameters of the eye plant (T_1, T_2, T_s), and determined the coefficients of determination obtained with the best-fit values of w_o. The best matches (maximum r^2) between predicted and actual eye speed were obtained when T_1, T_2 and T_s remained within 15% of their standard values, as indicated by the plots of r^2 values in Fig. 3. The optimal plant (i.e. the plant that the system appears designed to compensate for) using equally weighted Purkinje cell outputs has parameters (14, 202 and 76 ms for T_1, T_2 and T_s, respectively) that are very singular to those of the standard eye plant (16, 179 and 83 ms). When we compared the predicted eye speed obtained with this optimal plant to that produced with the standard plant, we found that the differences were probably due to chance ($Q > 0.99$). Together, these results argue that the population average of Purkinje cells is specifically tuned to compensate for the dynamics of the eye.

Finally, the compensation for eye dynamics generalizes to other eye speeds and across subjects. In each of the two monkeys, we recorded the firing rate of some Purkinje cells during pursuit eye movements at several different speeds. Using an equal weighting scheme ($w_s = 0$) and setting the single free parameter w, to fixed values of either 0.480 (monkey 1) or 0.436 (monkey 2). we obtained a set population averages for each monkey (Fig. 4a). Passing these population averages through the description of the standard eye plant again produced temporal profiles of eye speed that were good predictors of the actual movements (Fig. 4b). Because we used a single parameter to scale the firing rates across different speeds, these predictions assume that the firing rates of Purkinje cells scale linearly with eye speed and that their firing rates sum linearly. Overall, the predicted and actual eye speeds were highly correlated ($r^2 > 0.95$), although in some cases the discrepancies between predicted and actual eye speed could not be attributed to chance (Q sometimes < 0.05). The absence of a good fit between predicted and actual eye speed in these cases (10 deg/s for monkey 1 and 30 deg/s for monkey 2) argues that our strict assumption of linearity is likely an oversimplification. Indeed, an eye-velocity saturation non-linearity has previously been proposed for the pursuit system that might account for the small observed deviations between the predicted and actual eye speeds [16]. The likelihood that our sample did not include all Purkinje cells involved in the pursuit response might also explain these deviations.

DISCUSSION

These results directly support the idea that the cerebellum contains internal models that are used to predict and counteract the physical constraints encountered during movement. Our finding that the population activity of Purkinje cells in the ventral paraflocculus can compensate for the eye plant during pursuit shows that this region of the cerebellum could act as an inverse model to provide

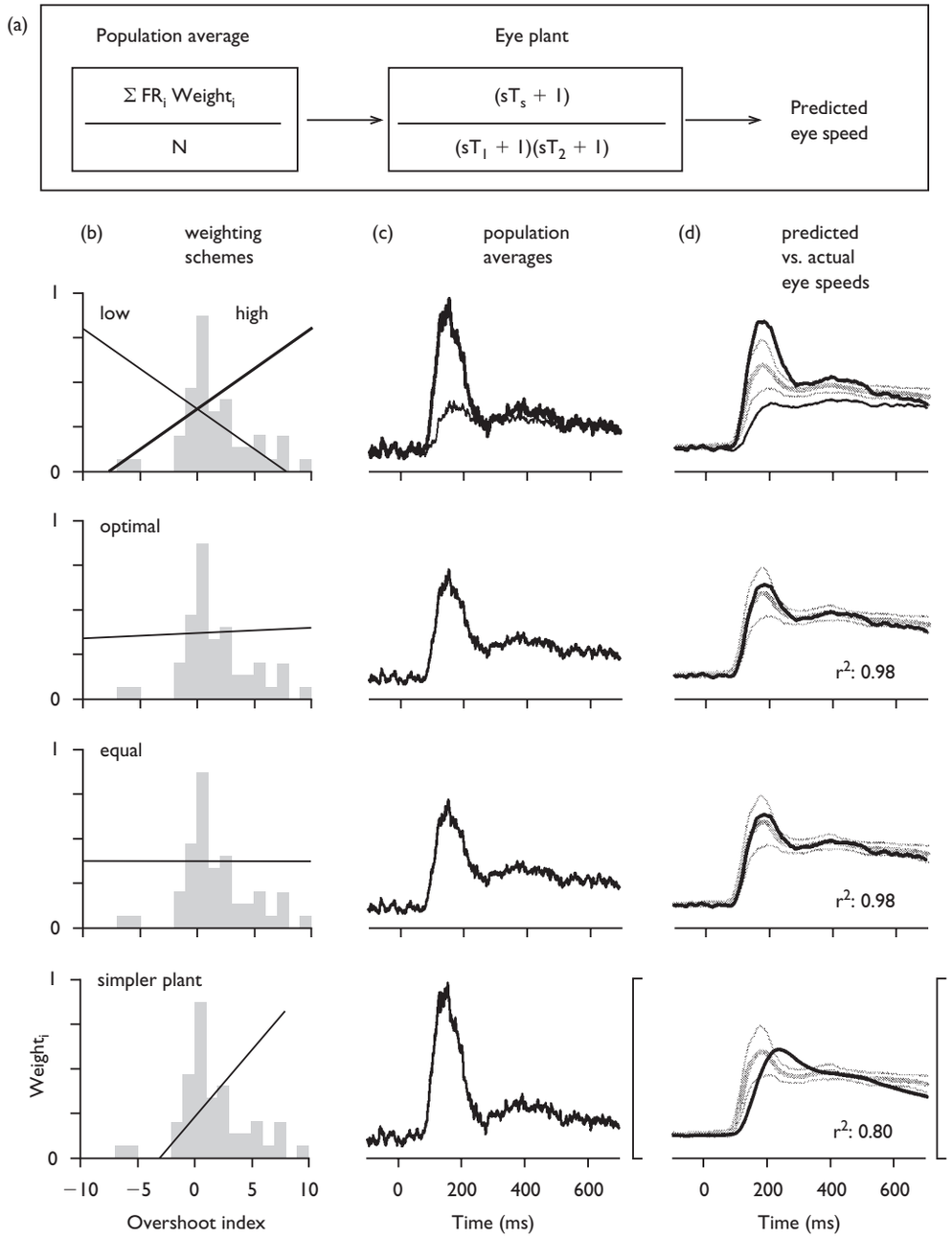

Fig. 2. Predicting pursuit eye movements with differently weighted averages of Purkinje cell firing. (**a**) The population average of Purkinje cell firing was passed through a second-order description of the eye plant to produce different predicted eye movements. The population average was obtained by scaling the firing rate of each Purkinje cell (FR_i) by a weight ($Weight_i$) defined by eqn (2), summing the resulting scaled firing rates, and dividing by the total number of Purkinje cells (N). The eye plant is described by a transfer function written in Laplace notation, consisting of one zero ($T_s = 83$ ms) and two poles ($T_1 = 16$ ms, $T_2 = 179$ ms). The input to the eye plant transfer function was the population average of Purkinje cell firing and the output was interpreted as predicted eye speed. Because this model uses Purkinje cell firing directly to drive the eye plant, it tests the assumption that no additional inputs or intervening neural dynamics are required to generate realistic pursuit. In most descriptions of the oculomotor pathways [13], the drive signal for the eye plant is mathematically integrated and the output of the eye plant is differentiated to obtain eye velocity. Because these integration and differentiation steps cancel, they were both omitted from the current model. (**b**) The different weighting schemes used to compute the population average. The shaded histogram reproduced in each row indicates the distribution of overshoot indices for the 50 Purkinje cells. The different lines in each row indicate five different weighting functions obtained from eqn (2) using different values of w_s and w_o, respectively: low (thin line), −0.045 and 0.35; high (thick line), 0.045 and 0.35; optimal, 0.003 and 0.37; equal, 0.0 and 0.376; and optimal: simpler plant, 0.074 and 0.24. (**c**) The five different population averages obtained using the five weighting functions described in (b). Bar = 25 spikes/s. (**d**) Comparisons between the predicted (solid) and actual (gray) temporal profiles of eye speed. Thin gray lines indicate 1 s.d. of the mean eye speed. r^2 values indicate the determination coefficients for the correlation between the predicted and actual eye speeds. Bar = 15 deg/s.

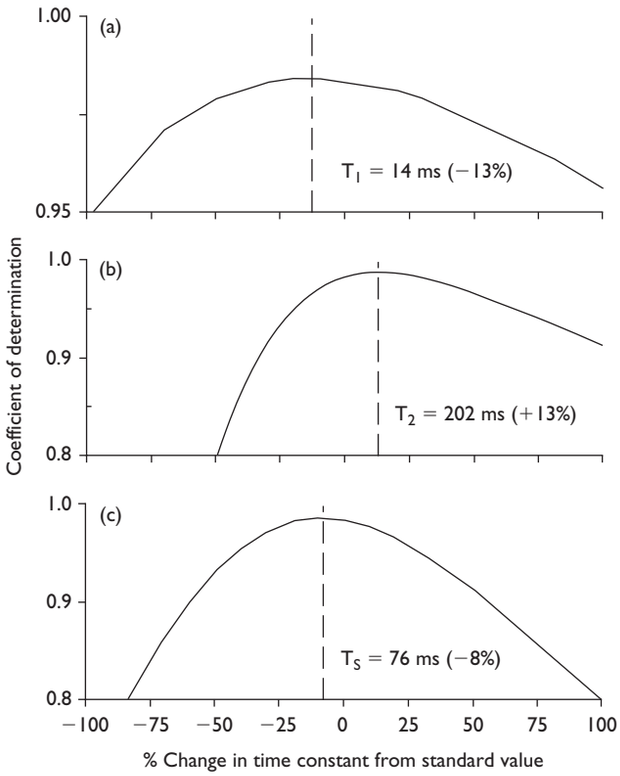

Fig. 3. Testing alternative models of the eye plant. The determination coefficient for the correlation between predicted and actual eye speeds is plotted against a range of values for each of the three time constants of the eye plant: T_1 (**a**), T_2 (**b**) and T_s (**c**). For each plotted point, we tested a different alternative plant by changing the values of T_1, T_2 or T_s by some percentage (± 100%) from their standard values of 16, 179 and 83 ms, respectively. For each alternative plant, the population average was constructed using an equal weighting scheme ($w_s = 0$), but the value of the weight w_o was optimized to produce the best fit. The dashed vertical lines and adjacent text indicate the time constant values that produced the highest correlation between predicted and actual eye speeds.

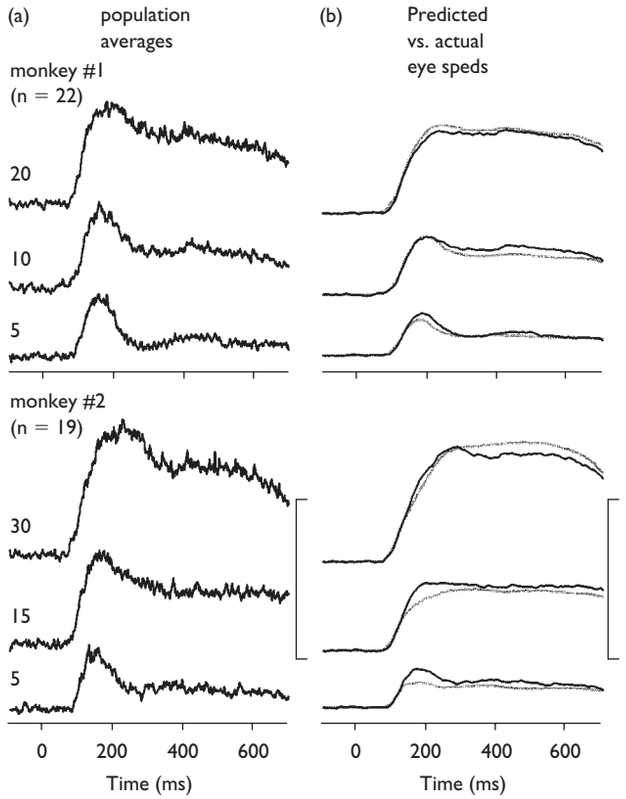

Fig. 4. Predicting a few speeds of pursuit eye movements with equally weighted averages of Purkinje cell firing. (**a**) The two sets of population averages obtained for each monkey during pursuit at the three different speeds indicated by the number to the left of each trace. Bar indicates 50 spike/s. (**b**) Comparisons between the predicted (solof each trace. Bar indicates 50 spike/s. (**b**) Comparisons between the predicted (solid) and actual (gray) temporal profiles of eye speed. The determination coefficients (r^2 values) were 0.99, 0.98, 0.98, 0.99, 0.99 and 0.96, for the six pairs of traces from top to bottom, respectively. The corresponding six Q scores (χ^2 test) were >0.99, <0.05, 0.93, <0.05, 0.30 and >0.99. Bar = 40 deg/s.

the motor commands needed to achieve desired smooth eye movements [18]. Previous studies of the ventral paraflocculus have shown that the temporal pattern of firing of single Purkinje cells can be reconstructed with a weighted sum of eye movement signals during ocular following [9,19]. These studies suggested the presence of a partial inverse dynamics representation, although not all of the coefficients required to fit the data were consistent with motor neuron firing. In particular, the position coefficient had a reversed sign, suggesting that additional signals from some other sources would be required to cancel the inappropriate position signals from the ventral paraflocculus. Notably, these studies omitted the slide component of motor neuron firing, which compensates for a lead element in the eye plant by contributing a filtered eye velocity command [17]. As our results show (Fig. 2d), omission of this term dramatically changes the relationship between Purkinje cell firing and predicted eye movements, and thus may have been at least partly responsible for the discrepant findings in these previous studies [9,19]. In another earlier study, using a model that included brain stem motor pathways as well as the eye plant, we showed that Purkinje cell activity could be used to predict the temporal profiles of pursuit eye velocity [11]. Our current results extend the above set of findings in three critical respects. First, by directly applying averages of Purkinje cell firing to the eye plant, our results demonstrate that the Purkinje cell population activity provides dynamic compensation without the need for additional inputs or processing. Second, by testing different weighting schemes, our results show that simply adding the firing rates of all Purkinje cells in the population achieves near-optimal compensation. Third, by testing alternative plants, our results indicate that this compensation is specifically tuned for the dynamics of the oculomotor plant.

Although the origin of this compensatory activity is not known, the absence of such activity on the eye movement inputs to the ventral paraflocculus [4,20] indicates that these signals are due to other, possibly visual, inputs to the cerebellum or to computations accomplished within the cerebellar cortex itself. Adaptive changes within the cerebellar circuitry [21,22] could make it possible to read out

the distributed activity of Purkinje cells with such a simple equal weighting scheme and still achieve appropriate dynamic compensation. Alternatively, by pooling Purkinje cells with unequal weights downstream of the cerebellum, it may be possible to quickly compensate for novel motor constraints. Finally, these results imply that accurate tracking can be achieved if the descending control signals from the cerebral cortex simply specify the motion of the target object, because compensation for motor constraints can be accomplished downstream. These data from the cerebellum therefore complement previous physiological and behavioral findings suggesting that information about visual and eye motion are integrated within extrastriate cortex (e.g., the medial superior temporal area) to provide a target motion signal for pursuit [23–25].

CONCLUSION

Our results demonstrate that an equally weighted average of Purkinje cell outputs can compensate for the dynamics of the eye during smooth tracking movements. These results address a general problem about brain function: how does the nervous system accomplish movements accurately, given the complex mechanical problems posed by biological components like muscles and connective tissue? Our findings suggest that the brain may indeed solve this problem by incorporating internal models of the body parts that are to be controlled.

REFERENCES

1. Westheimer G and Blair SM. *Exp Brain Res* **21**, 463–472 (1974).
2. Zee DS *et al. J Neurophysiol* **46**, 878–899 (1981).
3. Miles FA and Fuller JH. *Science* **189**, 1000– 1002 (1975).
4. Miles FA *et al. J Neurophysiol* **43**, 1437–1476 (198).
5. Lisberger SG and Fuchs AF. *J Neurophysiol* **41**, 733–777 (1978).
6. Stone LS and Lisberger SG. *J Neurophysiol* **63**, 1241–1261 (1990).
7. Krauzlis RJ and Lisberger SG. *Exp Brain Res* **109**, 289–302 (1996).
8. Krauzlis RJ and Lisberger SG. *Science* **253**, 568–571 (1991).
9. Shidara M *et al. Nature* **365**, 50–52 (1993).
10. Press WH *et al. Numerical Recipes in C The Art of Scientific Computing.* 1988, Cambridge: Cambridge University Press.
11. Krauzlis RJ and Lisberger SG. *J Neurophysiol* **72**, 2045–2050 (1994).
12. Keller EL. Accommodative vergence in the alert monkey. Motor unit analysis. Vision Res 13(8), 1565-75 (1973).
13. Robinson DA. Control of eye movements. In: Brooks VB, ed. *Handbook of Physiology, Section 1: The Nervous System.* Vol II, Part 2. Bethesda: Am Physiological Soc, 1981: 1275–1320.
14. Goldstein HP. The neural encoding of saccades in the rhesus monkey. PhD. Thesis, 1983, Johns Hopkins University, Baltimore, MD.
15. Fuchs AF, Scudder CA and Kaneko CRS. *J Neurophysiol* **60**, 1874–1895 (1988).
16. Robinson DA, Gordon JL and Gordon SE. *Biol Cybern* **55**, 43–57 (1986).
17. Optican LM and Miles FA. *J Neurophysiol* **54**, 940–958 (1985).
18. Wolpert DM, Miall RC and Kawato M. *Trends Cogn Sci* **2(8)**, 338–347 (1998).
19. Gomi H *et al. J Neurophysiol* **80**, 818–831 (1998).
20. Lisberger SG and Fuchs F. *J Neurophysiol* **41**, 764–777 (1978).
21. Marr D. *J Physiol (Lond.)* **202**, 437–470 (1969).
22. Albus JS. *Math Biosci* **10**, 25–61 (1971).
23. Newsome WT, Wurtz RH and Komatsu H. *J Neurophysiol* **60**, 604–620 (1988).
24. Stone LS, Beutter BR and Lorenceau J. On the visual input driving human smooth-pursuit eye movements. *NASA Technical Memorandum.* Washington DC: NASA, 1996.
25. Ilg UJ and Thier P. MST neurons are activated by smooth pursuit of imaginary targets, In: Thier P and Karnath H-O, eds. *Parietal Contributions to Orientation in 3D Space*, Springer-Verlag: Heildelberg, 1997: 173–184.